

# Gold nanocages covered by smart polymers for controlled release with near-infrared light

Mustafa S. Yavuz<sup>\*</sup>, Yiyun Cheng<sup>\*</sup>, Jingyi Chen<sup>\*</sup>, Claire M. Cobley, Qiang Zhang, Matthew Rycenga, Jingwei Xie, Chulhong Kim, Kwang H. Song, Andrea G. Schwartz, Lihong V. Wang and Younan Xia<sup>†</sup>

**Photosensitive caged compounds have enhanced our ability to address the complexity of biological systems by generating effectors with remarkable spatial/temporal resolutions<sup>1–3</sup>. The caging effect is typically removed by photolysis with ultraviolet light to liberate the bioactive species. Although this technique has been successfully applied to many biological problems, it suffers from a number of intrinsic drawbacks. For example, it requires dedicated efforts to design and synthesize a precursor compound for each effector. The ultraviolet light may cause damage to biological samples and is suitable only for *in vitro* studies because of its quick attenuation in tissue<sup>4</sup>. Here we address these issues by developing a platform based on the photothermal effect of gold nanocages. Gold nanocages represent a class of nanostructures with hollow interiors and porous walls<sup>5</sup>. They can have strong absorption (for the photothermal effect) in the near-infrared while maintaining a compact size. When the surface of a gold nanocage is covered with a smart polymer, the pre-loaded effector can be released in a controllable fashion using a near-infrared laser. This system works well with various effectors without involving sophisticated syntheses, and is well suited for *in vivo* studies owing to the high transparency of soft tissue in the near-infrared region<sup>6</sup>.**

Figure 1a shows a schematic of the controlled-release system. The Au nanocages are typically prepared by means of the galvanic replacement reaction between Ag nanocubes and HAuCl<sub>4</sub> or HAuCl<sub>2</sub> in water<sup>7</sup>. The polymer is based on poly(*N*-isopropylacrylamide) (pNIPAAm) and its derivatives, which can change conformation in response to small variations in temperature<sup>8</sup>. On exposure to a laser beam with a wavelength that matches the absorption peak of the Au nanocage, the light will be absorbed and converted into heat through the photothermal effect<sup>9,10</sup>. The heat will dissipate into the surroundings, and the rise in temperature will cause the polymer chains to collapse (see Supplementary Information for a detailed analysis), exposing the pores on the nanocage and thereby releasing the pre-loaded effector. When the laser is turned off, heating will immediately cease and the drop in temperature will bring the polymer back to its original, extended conformation, closing the pores and stopping the release. We can control the release dosage by manipulating the power density and/or irradiation time.

For pure pNIPAAm, its low critical solution temperature (LCST) is about 32 °C. Below 32 °C, the polymer is hydrophilic and soluble in water. When the temperature is raised above 32 °C, the polymer undergoes a phase transition to a hydrophobic state, generating turbidity owing to aggregation. Typically, the LCST is defined as the temperature at which the light transmission of the polymer

solution drops to 90% of the original value<sup>8</sup>. By incorporating acrylamide (AAm) into the polymer chain, we obtained pNIPAAm-*co*-pAAm copolymers with LCSTs being tuned to anywhere in the range of 32–50 °C (Supplementary Fig. S1 and Table S1; ref. 8). For *in vivo* applications, the LCST should be tuned to a value above the body temperature (37 °C) but below the hyperthermia temperature (42 °C). Here, we have focused on two types of polymer: pNIPAAm and a pNIPAAm-*co*-pAAm copolymer with an LCST at 32 and 39 °C, respectively. Both were prepared using atom-transfer radical polymerization<sup>11,12</sup>.

We covalently anchored the smart polymer to the surface of Au nanocages by means of gold-thiolate linkage. One way to achieve this is to include a disulphide bond in the middle of the polymer chain by using a disulphide initiator<sup>12</sup> (Fig. 1b). As thiolate has a stronger binding towards the Au surface than the C=O group of poly(vinyl pyrrolidone) (PVP), we could replace the PVP on nanocages with the smart polymer. After the displacement, the absorption peak of the nanocages redshifted by ~13 nm, which could be offset during the nanocage synthesis. As shown in Fig. 1c by transmission electron microscope (TEM) imaging, the pNIPAAm-*co*-pAAm coating had a relatively uniform thickness of ~3 nm in the dry state. This result is in reasonable agreement with the value (~5 nm) estimated from the thermogravimetric analysis and gel permeation chromatography data shown in Supplementary Fig. S2 and Table S1. By dynamic light scattering, the mean hydrodynamic diameter of the copolymer-covered nanocages was observed to oscillate in response to temperature variation (Supplementary Fig. S3): the diameter increased by 13% on cooling to 37 °C and shrank to its original value on heating to 41 °C. These changes with temperature were reversible. During cooling/heating, the polydispersity index of the sample remained less than 0.12, suggesting that no agglomeration occurred in the solution owing to the use of dilute samples.

To demonstrate the controlled release of medium-sized effectors from the copolymer-covered nanocages, we prepared alizarin-PEG by coupling the hydroxyl end group of poly(ethylene glycol) (PEG;  $M_w \approx 5,000$ ) with the carboxyl group of alizarin yellow acid<sup>13</sup>. The nanocages were added to an aqueous solution of alizarin-PEG (23 mM) and shaken at 42 °C to load the dye. After 12 h, the suspension was quickly cooled with an ice bath to trigger conformational change for the copolymer, closing the pores and keeping the loaded dye inside the nanocages. If the loaded sample was kept under ambient laboratory conditions, the dye remained in the nanocages with negligible release (Supplementary Fig. S4). However, when the sample was heated above the LCST (39 °C) of the copolymer, the dye would come out through the opened pores. Figure 2a shows the release profile when the sample was

Department of Biomedical Engineering, Washington University, St Louis, Missouri 63130, USA. \*These three authors contributed equally to this project.

<sup>†</sup>e-mail: xia@biomed.wustl.edu.

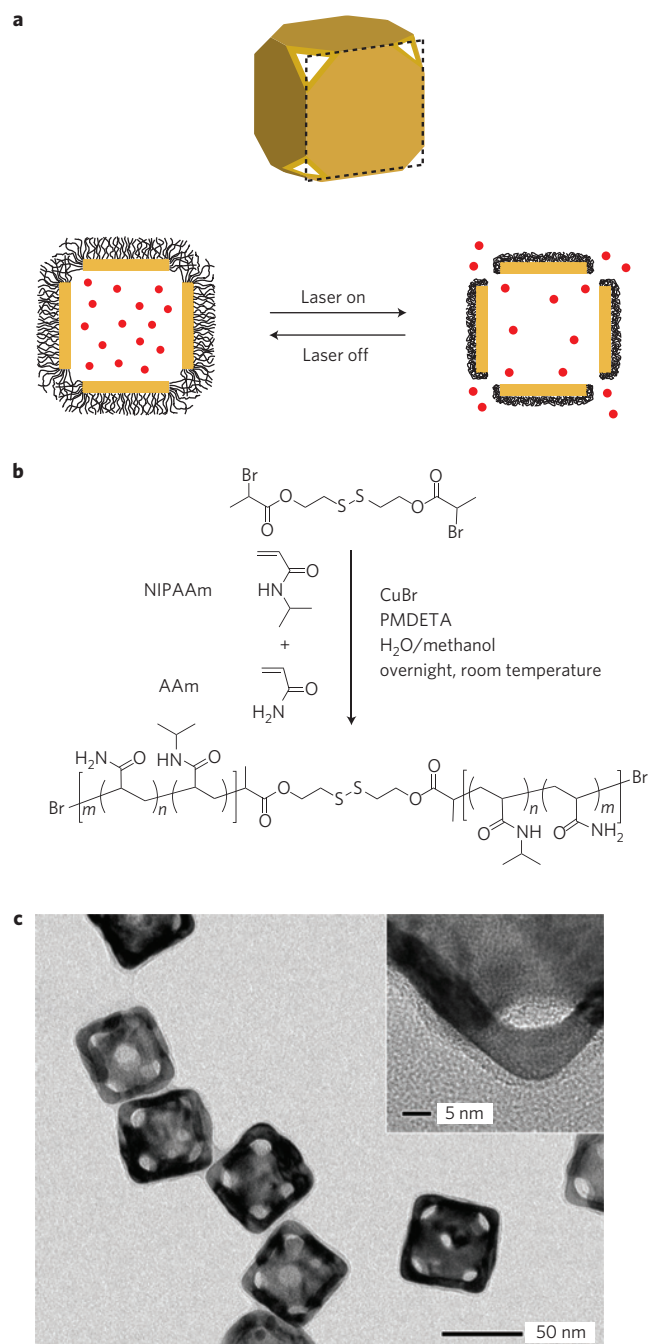


**Figure 1 | Schematic illustration and characterization of the controlled-release system.**

**a**, Schematic illustrating how the system works. A side view of the Au nanocage is used for the illustration. On exposure to a near-infrared laser, the light is absorbed by the nanocage and converted into heat, triggering the smart polymer to collapse and thus release the pre-loaded effector. When the laser is turned off, the polymer chains will relax back to the extended conformation and terminate the release. **b**, Atom-transfer radical polymerization of NIPAAm and AAm monomers (at a molar ratio of  $m/n$ ) as initiated by a disulfide initiator and in the presence of a Cu(I) catalyst. **c**, TEM images of Au nanocages for which the surface was covered by a pNIPAAm-co-pAAm copolymer with an LCST at 39 °C. The inset shows a magnified TEM image of the corner of such a nanocage.

heated at 42 °C for different periods of time. As alizarin-PEG has an absorption peak at 354 nm, its release could be easily monitored by recording ultraviolet–visible spectra of the supernatants

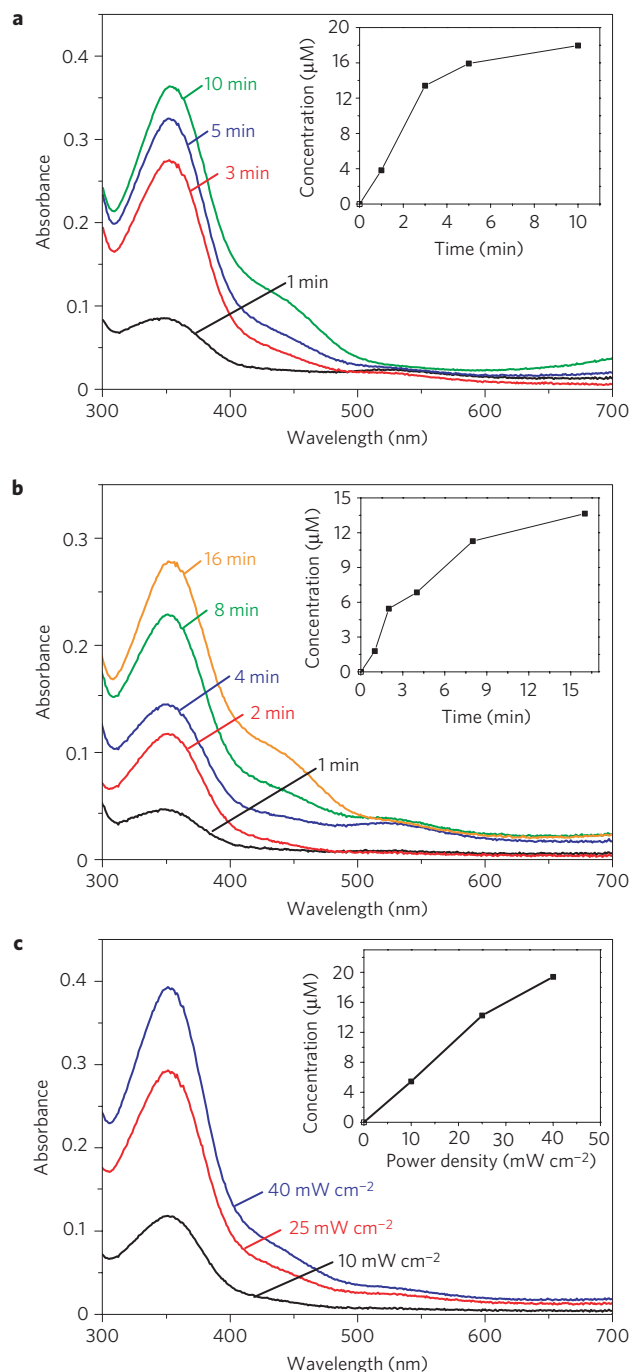


**Figure 2 | Controlled release of a dye from the Au nanocages covered by a copolymer with an LCST at 39 °C.**

**a–c**, Absorption spectra of alizarin-PEG released from the copolymer-covered Au nanocages by heating at 42 °C for 1, 3, 5 and 10 min (**a**); by exposure to a pulsed near-infrared laser at a power density of 10 mW cm<sup>-2</sup> for 1, 2, 4, 8 and 16 min (**b**); and by exposure to the near-infrared laser for 2 min at 10, 25 and 40 mW cm<sup>-2</sup> (**c**). The insets show the concentrations of alizarin-PEG released from the nanocages under different conditions.

at different times after the nanocages had been centrifuged down. As heating was prolonged, the amount of alizarin-PEG released into the solution kept increasing, and eventually levelled off. By referring to a calibration curve separately prepared for the same dye, we determined the exact concentration of alizarin-PEG released from the nanocages at different times, as shown in the inset of Fig. 2a.

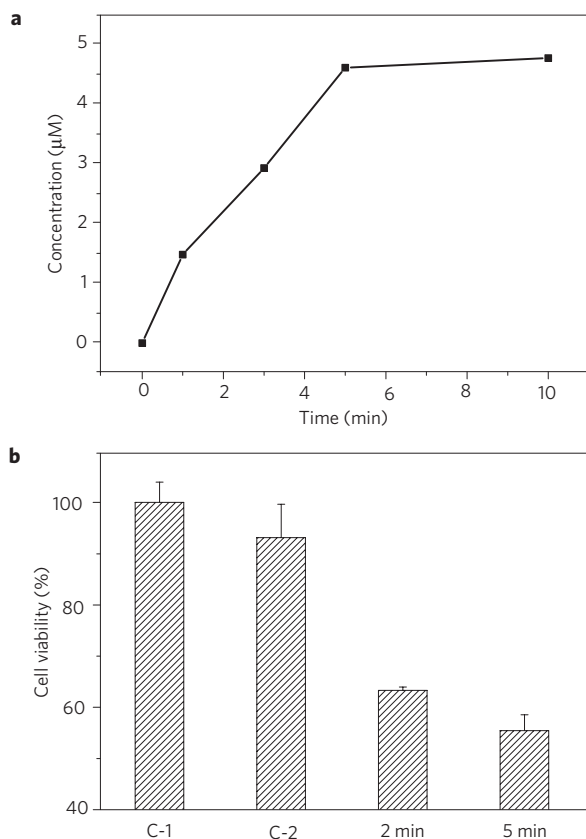


**Figure 3 | Controlled release of an anticancer drug from the Au nanocages covered by a copolymer with an LCST at 39 °C.** **a**, A plot of the concentrations of Dox released from the Au nanocages on heating at 45 °C for different periods of time. **b**, Cell viability for samples after going through different treatments: (C-1) cells irradiated with a pulsed near-infrared laser for 2 min in the absence of Au nanocages; (C-2) cells irradiated with the laser for 2 min in the presence of Dox-free Au nanocages; and (2/5 min) cells irradiated with the laser for 2 and 5 min in the presence of Dox-loaded Au nanocages. A power density of 20 mW cm<sup>-2</sup> was used for all of these studies.

We also controlled the release with a near-infrared laser by means of the photothermal effect. For this purpose, the suspension of dye-loaded nanocages was exposed to a Ti:sapphire laser at 10 mW cm<sup>-2</sup> for different periods of time. Under this condition, most of the dye molecules were released within 16 min (Fig. 2b). We also tested the dependence of dye release on the power density when the time was kept at 2 min. As shown in Fig. 2c, because more heat was generated at a higher power density, the pores were forced to open for a longer period of time. Therefore, higher power density caused more release of alizarin-PEG from the nanocages. Note that the Au nanocages started to melt at a power density of 40 mW cm<sup>-2</sup> (Supplementary Fig. S5), a phenomenon that was also observed in previous studies<sup>14–16</sup>, indicating that a laser power density below 40 mW cm<sup>-2</sup> should be used if one wants to reload the Au nanocages with chemical species. We did demonstrate the capability to reuse the smart capsules that were used for Fig. 2b after laser-triggered release. In this case, the used nanocages were washed with warm water (42 °C) three times to remove all possibly trapped dye. We then reloaded the nanocages with alizarin-PEG, followed by release with heating. As shown in Supplementary Fig. S6, we obtained a total amount of release essentially the same as the first-round release experiment. This result confirms that the Au nanocages were not melted nor were the polymer chains desorbed from the nanocage surface during a

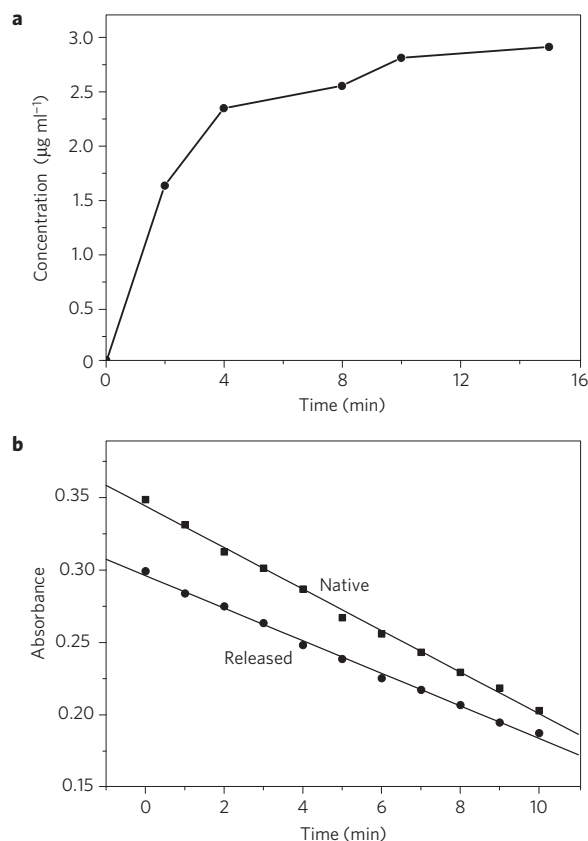


**Figure 4 | Controlled release of an enzyme from the Au nanocages covered by pNIPAAm with an LCST at 32 °C.** **a**, A plot of the concentrations of lysozyme released from the Au nanocages on heating at 37 °C for different periods of time. **b**, Lysozyme bioactivity test. Linear fit ( $y$ : absorbance,  $x$ : time) for native lysozyme:  $y = -0.014x + 0.34$ ,  $R^2 = 0.99$  and linear fit for the released lysozyme:  $y = -0.011x + 0.34$ ,  $R^2 = 0.99$ .

laser-triggered release experiment (see Supplementary Information for a detailed discussion).

We further extended the controlled release to an *in vitro* study that involved killing of breast cancer cells with doxorubicin (Dox), a commercial chemotherapeutic drug for breast cancer<sup>17</sup>. The Dox release profile (Fig. 3a) from the copolymer-covered nanocages was similar to what was observed for the dye (Fig. 2a). We observed a fast release of Dox when the sample was subjected to heating. It has been shown that the presence of Dox at a micromolar level (µM) can cause breast cancer cells to die and thus provide a simple readout. In a typical study, the cancer cells were seeded in a 24-well plate and allowed to proliferate until reaching 80% confluence. The wells containing cancer cells and Dox-loaded nanocages were irradiated with the Ti:sapphire laser at a power density of 20 mW cm<sup>-2</sup> for 2 and 5 min, respectively, and the data are plotted in Fig. 3b. As the irradiation time increased, more cancer cells were observed to die because more Dox was released. In comparison, laser irradiation on sample C-1 in the absence of Au nanocages had essentially no effect on cell viability. Laser irradiation on sample C-2 in the presence of Au nanocages alone resulted in a slight reduction in viability, probably owing to the photothermal effect of Au nanocages<sup>9,18</sup>. These results are consistent with the drug release data shown in Fig. 3a. In practice, parameters including cage concentration, drug loading, laser irradiation time and power density all need to be optimized to further improve the efficacy of killing cancer cells.

An enzyme was also used to test encapsulation and controlled release. In this case, we used a lysozyme that can damage the cell

walls of bacteria by catalysing the hydrolysis process<sup>19</sup>. To maintain the enzyme activity, we used pNIPAAm with an LCST of 32 °C. The lysozyme was released by heating the system to 37 °C, as was the case for the dye. Concentrations of the released lysozyme, shown in Fig. 4a, were quantified using the Micro BCA protein assay<sup>20</sup>. The maximum concentration released (2.91  $\mu\text{g ml}^{-1}$ ) from the Au nanocages was close to the value (3.88  $\mu\text{g ml}^{-1}$ ) calculated from the initial concentration of the loading solution and the volume ratio of Au nanocages to the suspension medium. The bioactivity of the released lysozyme was determined from the rate of lysis for *Micrococcus lysodeikticus* cells. As shown in Fig. 4b, the released lysozyme was able to maintain ~80% of the bioactivity after going through the encapsulation and release processes. This bioactivity is relatively high compared with the typical values (30–80%) reported for other encapsulation schemes<sup>21–23</sup>.

We have demonstrated a platform based on Au nanocages covered with smart polymers for controlled release with near-infrared light. When combined with optical manipulation (for example, trapping<sup>24</sup>), this platform offers many extra advantages such as high spatial/temporal resolutions. In addition, Au nanocages are bio-inert and the surface can be readily functionalized with targeting ligands such as antibodies using the gold-thiolate chemistry<sup>25,26</sup>.

## Methods

**Polymerization of NIPAAm and AAm.** NIPAAm (2.0 g), *N,N,N',N',N'*-pentamethyldiethylenetriamine (PMDETA) (35  $\mu\text{l}$ ), *bis*(2-hydroxyethyl)disulphide *bis*(2-bromopropionate) (0.015 g), deionized water (18 ml) and methanol (12 ml) were mixed in a Schlenk flask and degassed by freeze–pump–thaw cycles. While the mixture was frozen, CuBr (0.010 g) was added. The flask was then filled with argon and the mixture was left to melt at room temperature. The reaction solution was magnetically stirred overnight at room temperature. After evaporation of the solvent, the crude product was dissolved in water and purified by dialysis to yield pNIPAAm. For copolymers, the same procedure was used except that the initial monomers were added as follows: (1) NIPAAm (95%, 1.93 g) and AAm (5%, 0.64 g) for an LCST at 35 °C; (2) NIPAAm (90%, 1.83 g) and AAm (10%, 0.13 g) for an LCST at 39 °C; (3) NIPAAm (87.5%, 1.78 g) and AAm (12.5%, 0.16 g) for an LCST at 41 °C; (4) NIPAAm (75%, 1.53 g) and AAm (25%, 0.32 g) for an LCST at 49 °C.

**Preparation of gold nanocages.** Gold nanocages were synthesized by means of the galvanic replacement reaction between truncated Ag nanocubes and chloroauric acid (HAuCl<sub>4</sub>). The synthetic procedures were described in detail in a recently published protocol<sup>27</sup>. For all of the experiments, we used Au nanocages of 50 nm in edge length together with a pore size of 5–10 nm. Sulphide-mediated polyol reduction was used to synthesize the Ag nanocubes and the procedure can be found in our previous publications<sup>27,28</sup>.

**Exchange of PVP with pNIPAAm or copolymer.** The as-synthesized PVP-covered Au nanocages were dispersed in 2 ml of deionized water and added to a 20 ml aqueous solution of pNIPAAm (0.20 g) or a copolymer (0.20 g). The mixture was shaken at 800 rpm for five days. The solution was then centrifuged at 14,000 rpm and the supernatant was discarded. The polymer-covered Au nanocages were washed three more times with 2 ml (each time) of deionized water.

**Loading the nanocages with alizarin-PEG, Dox or lysozyme.** The alizarin-PEG, Dox and lysozyme solutions were freshly prepared and directly used with the nanocages. The polymer-covered nanocages were added to an aqueous solution (1 ml) containing alizarin-PEG (0.12 g), Dox (0.020 g) or lysozyme (0.25 g). The mixture was shaken overnight at 1,000 rpm at 37 °C for pNIPAAm-covered nanocages and at 42 °C for copolymer-covered nanocages, respectively. The mixture was then cooled with an ice bath for 1 h, and centrifuged at 14,000 rpm for 20 min. Finally, the supernatant was decanted and the loaded samples were washed eight more times with 1.5 ml (each time) of deionized water.

**Releasing alizarin-PEG from gold nanocages by heating.** Before alizarin-PEG release, the loaded nanocages were centrifuged down and the supernatant was decanted. Warm (42 °C) water (0.5 ml) was added to the sample, followed by incubation under vortexing in a 42 °C water bath for different periods of time. Then, the solution was cooled with an ice bath for 5 min, followed by centrifugation at 14,000 rpm and 20 °C for 10 min. The supernatant was then taken for ultraviolet–visible spectral measurement.

**Releasing alizarin-PEG from gold nanocages by laser.** For each data point, 0.5 ml of the alizarin-PEG-loaded nanocages was prepared and transferred to a 1.5-ml centrifuge tube. The sample was pre-heated in a shaking incubator at 37 °C to mimic the body temperature before laser irradiation. Each sample was

exposed to the Ti:sapphire laser for different periods of time at a fixed power density of 10 mW cm<sup>-2</sup>, or for 2 min at power densities of 10, 25 and 40 mW cm<sup>-2</sup>. After exposure, the solution was centrifuged at 14,000 rpm for 20 min, and the supernatant was collected for ultraviolet–visible spectral measurement.

**Releasing lysozyme from gold nanocages by heating.** We used the same procedure described for the release of alizarin-PEG except that the release temperature was set to 37 °C.

**Calculating the concentration of released lysozyme.** Native lysozyme was dissolved in Dulbecco's PBS to obtain solutions of 0.5, 1, 2.5, 5, 10, 20, 40 and 200  $\mu\text{g ml}^{-1}$  in concentration. Micro BCA Protein Assay (1 ml) was added to 1 ml of the lysozyme sample with a known (native) or an unknown (released from the nanocages) concentration. The culture tubes were incubated at 60 °C for 1 h and then examined with a spectrometer. For the known samples, we could obtain a calibration curve by plotting the absorbance at 562 nm against the concentration of lysozyme. The unknown concentrations of the released lysozyme were then determined from the calibration curve.

Received 5 February 2009; accepted 30 September 2009;  
published online 1 November 2009

## References

- Adams, S. R. & Tsien, R. Y. Controlling cell chemistry with caged compounds. *Annu. Rev. Physiol.* **55**, 755–784 (1993).
- Kramer, R. H., Chambers, J. J. & Trauner, D. Photochemical tools for remote control of ion channels in excitable cells. *Nature Chem. Bio.* **7**, 360–365 (2005).
- Mayer, G. & Heckel, A. Biologically active molecules with a light switch. *Angew. Chem. Int. Ed.* **45**, 4900–4921 (2006).
- Schwarz, A. *et al.* Interleukin-12 suppresses ultraviolet radiation-induced apoptosis by inducing DNA repair. *Nature Cell Bio.* **4**, 26–31 (2002).
- Chen, J. *et al.* Facile synthesis of gold-silver nanocages with controllable pores on the surface. *J. Am. Chem. Soc.* **128**, 14776–14777 (2006).
- Weissleder, R. A clearer vision for *in vivo* imaging. *Nature Biotechnol.* **19**, 316–317 (2001).
- Skrabalak, S. E. *et al.* Gold nanocages: Synthesis, properties, and applications. *Acc. Chem. Res.* **41**, 1587–1595 (2008).
- Hoffman, A. S. Hydrogels for biomedical applications. *Adv. Drug Deliv. Rev.* **43**, 3–12 (2002).
- Au, L. *et al.* A quantitative study on the photothermal effect of immuno gold nanocages targeted to breast cancer cells. *ACS Nano* **2**, 1645–1652 (2008).
- Liu, G. L., Kim, J., Lu, Y. & Lee, L. P. Optofluidic control using photothermal nanoparticles. *Nature Mater.* **5**, 27–32 (2005).
- Jonas, A. M., Hu, Z., Gline, K. & Huck, W. T. S. Effect of nanoconfinement on the collapse transition of responsive polymer brushes. *Nano Lett.* **8**, 3819–3824 (2008).
- Tsarevsky, N. V. & Matyjaszewski, K. Combining atom transfer radical polymerization and disulphide/thiol redox chemistry: A route to well-defined (bio)degradable polymeric materials. *Macromolecules* **38**, 3087–3092 (2005).
- Li, H., Jerome, R. & Lecomte, P. Amphiphilic sun-shaped polymers by grafting macrocyclic copolyesters with PEO. *Macromolecules* **41**, 650–654 (2008).
- Hu, M. *et al.* Ultrafast laser studies of the photothermal properties of gold nanocages. *J. Phys. Chem. B* **110**, 1520–1524 (2006).
- Link, S., Wang, Z. L. & El-Sayed, M. A. How does a gold nanorod melt? *J. Phys. Chem. B* **104**, 7867–7870 (2000).
- Wu, G. *et al.* Remotely triggered liposome release by near-infrared light absorption via hollow gold nanoshells. *J. Am. Chem. Soc.* **130**, 8175–8177 (2008).
- Wu, E. C. *et al.* Oxidation-triggered release of fluorescent molecules or drugs from mesoporous Si microparticles. *ACS Nano* **2**, 2401–2409 (2008).
- Chen, J. *et al.* Immuno gold nanocages with tailored optical properties for targeted photothermal destruction of cancer cells. *Nano Lett.* **7**, 1318–1322 (2007).
- Ghaderi, A. & Carlfors, J. Biological activity of lysozyme after entrapment in poly(d,l-lactide-co-glycolide) microspheres. *Pharm. Res.* **14**, 1556–1562 (1997).
- Xie, J. & Wang, C.-H. Encapsulation of proteins in biodegradable polymeric microparticles using electrospray in the Taylor cone-jet mode. *Biotechnol. Bioeng.* **97**, 1278–1290 (2007).
- Kang, F., Jiang, G., Hinderliter, A., Deluca, P. P. & Singh, J. Lysozyme stability in primary emulsion for PLGA microsphere preparation: Effect of recovery methods and stabilizing excipients. *Pharm. Res.* **19**, 629–633 (2002).
- Srinivasan, C., Katara, Y. K., Muthukumar, T. & Panda, A. K. Effect of additives on encapsulation efficiency, stability, and bioactivity of entrapped lysozyme from biodegradable polymer particles. *J. Microencapsul.* **22**, 127–138 (2005).
- Weert, M. V. D., Hoechstetter, J., Hennink, W. E. & Crommelin, D. J. A. The effect of a water/organic solvent interface on the structural stability of lysozyme. *J. Controlled Release* **68**, 351–359 (2000).

24. Hansen, P. M., Bhatia, V. K., Harrit, N. & Oddershede, L. Expanding the optical trapping range of gold nanoparticles. *Nano Lett.* **5**, 1937–1942 (2005).
25. Love, J. C., Estroff, L. A., Kriebel, J. K., Nuzzo, R. G. & Whitesides, G. M. Self-assembled monolayers of thiolates on metals as a form of nanotechnology. *Chem. Rev.* **105**, 1103–1170 (2005).
26. Chen, J. *et al.* Gold nanocages: Bioconjugation and their potential use as optical imaging contrast agents. *Nano Lett.* **5**, 473–477 (2005).
27. Skrabalak, S. E., Au, L., Li, X. & Xia, Y. Facile synthesis of Ag nanocubes and Au nanocages. *Nature Protocols* **2**, 2182–2190 (2007).
28. Siekkinen, A. R., McLellan, J. M., Chen, J. & Xia, Y. Rapid synthesis of small silver nanocubes by mediating polyol reduction with a trace amount of sodium sulfide or sodium hydrosulfide. *Chem. Phys. Lett.* **432**, 491–496 (2006).

### Acknowledgements

This work was supported by a 2006 Director's Pioneer Award from the NIH (DP1 OD000798). Part of the work was carried out at the Nano Research Facility (NRF), a member of the National Nanotechnology Infrastructure Network (NNIN),

which is supported by the NSF under award no. ECS-0335765. NRF is part of School of Engineering and Applied Science at Washington University in St Louis.

### Author contributions

M.S.Y. and Y.C. synthesized the alizarin-PEG dye and polymers, carried out the loading and controlled-release experiments and did data analysis. J.C., C.M.C. and A.G.S. carried out the synthesis, surface modification and characterization of Au nanocages. C.M.C. and Q.Z. synthesized the Ag nanocubes. M.R. analysed the mechanism for laser-triggered release. C.K., K.H.S. and L.V.W. were involved in the planning of laser-triggered release experiments and helped with the analysis on Au nanocage melting. J.C. and J.X. conducted the cell viability, protein assay and enzyme activity assays. Y.X. conceived the strategy, supervised the experiments and prepared different versions of the manuscript.

### Additional information

Supplementary information accompanies this paper on [www.nature.com/naturematerials](http://www.nature.com/naturematerials). Reprints and permissions information is available online at <http://npg.nature.com/reprintsandpermissions>. Correspondence and requests for materials should be addressed to Y.X.